EFFECTS OF "CHEVRON" PARTITIONING ON SPATIALLY-EVOLVING MIXING LAYERS

***S. Lardeau*[1] *and S. Laizet*[1]**

[1] ***Imperial College London, Department of Aeronautics, SW7 2AZ***

s.lardeau@imperial.ac.uk

Abstract

The effect of streamwise-oriented perturbations on the spatial development of a mixing layer, is investigated using Direct Numerical Simulation. The streamwise vortices are generated downstream of a jagged partition. The variation of the chevrons wavelength is found to have a first-order effect on the growth rate of the mixing layer. Two different chevron-spanwise length are considered, as well as two different trailing-edge thicknesses. Results are compared with "natural" cases, obtained using a straight trailing edge (i.e. without spanwise excitation). The streamwise vortices are found to affect the mixing layer far downstream of the trailing edge, for a particular combination of chevrons length and plate thickness.

1 Introduction

Reducing aircraft noise during take-off and landing phases is one of the targets set by ACARE for 2020. One of the main source of noise is the flow coming out of jet nozzle itself. A possible design used to reduce such noise is to modified the nozzle by introducing a jagged partition between the main and the bypass exhaust, i.e. by forcing specific type of instabilities. Stability analysis have shown that two types of spanwise instabilities are competing during the early stage of a free-shear layer (Schoppa et al, 1995): translative (bending) and bulging, and these instabilities lead to the occurence of 3D flow structures. However, all physical processes at play are still not clearly understood. Indeed, several recent simulations have shown that the streamwise evolution of free-shear flows downstream of the trailing-edge can be greatly influenced by the thickness of the splitter plate (Laizet et al, 2010). The resulting large-scale, high-energy, structures are associated with two important physical phenomena: mixing enhancement and noise generation. The present work will attempt to address some of these questions by undertaking Direct Numerical Simulations (DNS) of free-shear flows created downstream of a jagged splitter plate.

This work follows several recent experiments conducted on chevron-partioned splitter plate (Kit et al 2007, Kit and Wignansky 2008, Zakharin et al 2009). In those works, the jagged partition triggers 3D instabilities in the free shear layers, and such instabilities are strongly modifying the development of the shear layer. Zakharin et al. (2009), for instance, have conjectured about the existence of counter-rotating vortices close to the trailing edge, and about their influence on the flow further downstream. Kit et al. (2007) have shown that, for stationery chevrons, significant differences were found between the momentum thickness downstream of the chevron's notch and that downstream of the cusp of the chevron.

The importance of streamwise streaks, imposed upstream of the splitter plate, has been conjectured by several authors (Lasheras & Choi, 1988). The problem is becoming more complex by the fact that, in the very early stage of the mixing layer development, the flows evolves from a wake-dominated instability to a mixing-layer instability. Several authors (e.g. Wallace and Redekopp, 1992) have found that the stability properties of the free-shear layer depends greatly on the upstream conditions (boundary layer thicknesses, velocity ratio, etc...).

In this paper, simulations of four different spatially-developing mixing layers, are performed. Two different modification of the baseline flow are considered: (i) the spanwise wavelength excitation and (ii) the splitter-plate thickness. The first part has already been partly explored by previous authors, and a strong dependence has been found for specific wavelength (of the order of the most-amplified excitation wavelength of 2/3 of the streamwise vortices spacing). For the second part, the behaviour is much less known, and indeed, only recently has the effect of splitter plate thickness been studied, both numerically (Laizet et al, 2010) and theoretically (Wallace and Redekopp, 1992). The main originality of this work is that the trailing-edges are specifically taken into account, using an Immersed Boundary Method. The flow configurations and the numerical methods are presented in Sections and , respectively, and results are given in Section . Main conclusions and under-going work are then detailed in Section

2 Flow configurations

We consider here the general flow configuration where two independent streams of velocity $U_1 = 1.2U_c$ and $U_2 = 0.8U_c$, with U_c being the

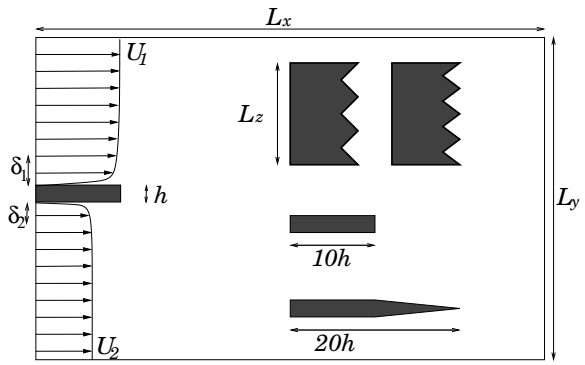

Figure 1: Flow configuration and nomenclature for the simulation with and without chevrons.

mean convection velocity, are flowing on opposite sides of a semi-infinite plate of thickness h (Figure 1). The inflow condition consists in two laminar boundary layers, of respective thickness $\delta_1 = 0.57h$ and $\delta_2 = 0.5h$. Low-amplitude time and space coherent perturbations are superimposed on the mean profiles. Domain dimensions and discretizations are similar to those used in Laizet et al. (2010): $(L_x, L_y, L_z) = (108h, 96h, 13.5h)$ and $(n_x, n_y, n_z) = (961, 257, 120)$. The outflow boundary condition is a simple convection equation, which has minimal upstream effect, due to the very convective nature of the flow. Periodicity is used in the z-direction and the grid is stretched in the y-direction in order to limit the confinement effects. The Reynolds number, based on the mean convection U_c and the initial step height h is $Re_h = 1000$.

Two chevrons spanwise wavelength are used: $\lambda_c = 4.5h$ and $\lambda_c = 3.375h$. The axis origin, for all cases, is located at the splitter plate trailing edge, and at cusp of the left-most chevron. Hence, the flow developing from the notch will be shifted compare to that developing from the cusp by a distance equal to the of the chevrons depth.

3 Numerical methods

The incompressible Navier-Stokes equations are solved using an in-house code (*Incompact3d*), based on sixth-order compact schemes for spatial discretization and second-order Adams-Bashforth scheme for time advancement. The Poisson equation is solved in Fourier space using the modified wave number formalism. The divergence-free condition is solved up to machine accuracy and this method allows more freedom in defining the boundary conditions (free-slip, periodic and Dirichlet boundary conditions). The different geometries for the jagged trailing edge are imposed using an Immersed Boundary Method (IBM) (Figure 1). Following the procedure proposed by Parnaudeau et al. (2008), the present IBM is a direct forcing approach that ensures the no-slip boundary condition at fluid-solid body interface. Combined with a sixth-order compact filtering of the convective terms, this specific IBM leads to a reduction of wiggles in the neighbourhood of the body, while allowing better quantitative predictions at marginal resolutions. The pressure mesh is staggered from the velocity one to avoid spurious pressure oscillations introduced by the IBM. More details about the present code and its validation, especially about the original treatment of the pressure in spectral space, can be found in Laizet and Lamballais (2009).

4 Results

Flow visualisation

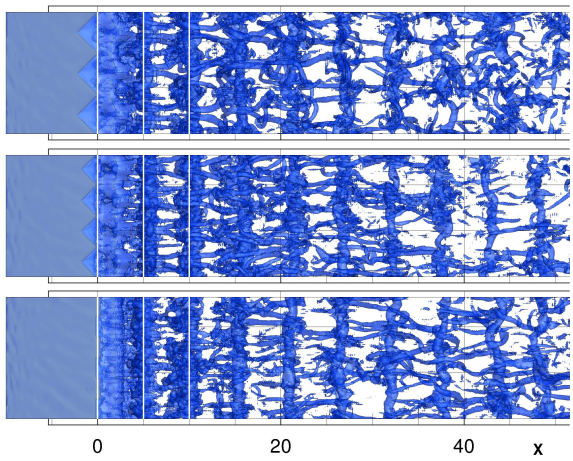

Figure 2: Top view of isosurfaces of the vorticity modulus $||\omega|| = 1U/h$ for all blunt trailing-edge cases and for, from top to bottom, $\lambda_c = 4.5h$, $\lambda_c = 3.375h$ and straight configuration. Only upstream part of the domain is shown. White lines indicate position of slices shown on Figures 9 and 10.

Instantaneous snapshots of isosurfaces of the vorticity modulus are shown on Figures 2 and 3 for the blunt and thin cases, respectively, and only for the first part of the domain. For the blunt case (Figure 2), the natural case shows that the flow becomes three-dimensional rapidly downstream. This was attributed to the strong wake-effect downstream of a "thick" splitter plate (Perret et al. 2005, Laizet et al. 2010). The size and intensity of those vortices is however weak, and they are dissipated (stretching) quickly. The flow is also dominated by large spanwise rollers. When the chevrons are introduced, the flow presents the same characteristic (large spanwise vortices, with numerous streamwise vortices generated between them). However, their spanwise spacing is increased, as it seems to be dictated by the chevron's spacing, and their intensity is also increased compare to the natural case. Indeed, well before the end of the domain, for the largest spanwise spacing, the spanwise vortices have disappeared, and the flow

has become three-dimensional. Hence, the main effect is seen on the creation of very intense streamwise vortices (braids) between the Kelvin-Helmholtz-like rollers, leading to an early breakdown of those rollers. Creation of streamwise vorticity on the flow

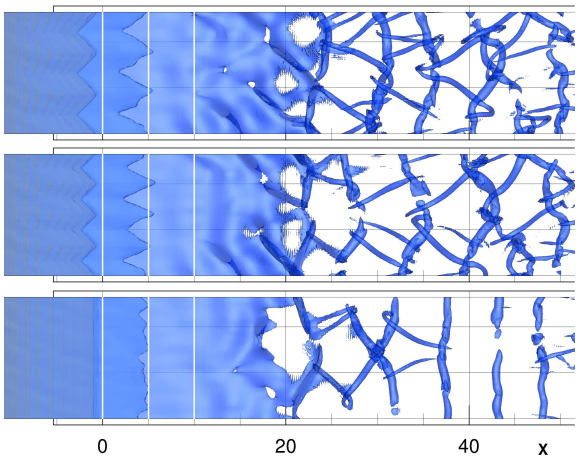

Figure 3: Top view of isosurfaces of the vorticity modulus $||\omega|| = 1U/h$ for all thin trailing-edge cases and for, from top to bottom, $\lambda_c = 4.5h$, $\lambda_c = 3.375h$ and straight configuration. Only upstream part of the domain is shown.

development is much more subtle for the thin trailing-edge case (fig. 3). However, it appears that the flow transitions quicker with a jagged partition.

Statistics

The streamwise evolution of the momentum thickness for the baseline case and for the $\lambda_c = 3.375h$ and $\lambda = 4.5h$ cases, for both blunt and thin trailing edges, are shown on Figure 4 and 5. Here, following Kit et al.(2007), the momentum thickness is defined as

$$\theta = \int_{-\infty}^{+\infty} \left(\frac{U - U_2}{U_1 - U_2}\right)\left(1 - \frac{U - U_2}{U_1 - U_2}\right) dy \quad (1)$$

where U is the mean streamwise velocity component. It is preferred to the definition used classically to study mixing layer, i.e. the vorticity thickness:

$$\delta = \frac{\partial U}{\partial y}_{max} \quad (2)$$

The last definition does not appear to be suitable in the very early development of the mixing layer, as two local maxima are present, for the two shear layers developing on each side of the splitter plate. The recirculation and the wake-deficit regions can indeed be consequent, and extend far downstream (Laizet et al., 2010). The flow is not homogeneous any more in spanwise direction, hence the momentum thickness on both the notch and the cusp for the jagged partition are shown, together with the momentum thickness obtained for the baseline case. Also shown on Figure 4 is the evolution of the mean flow deficit on the

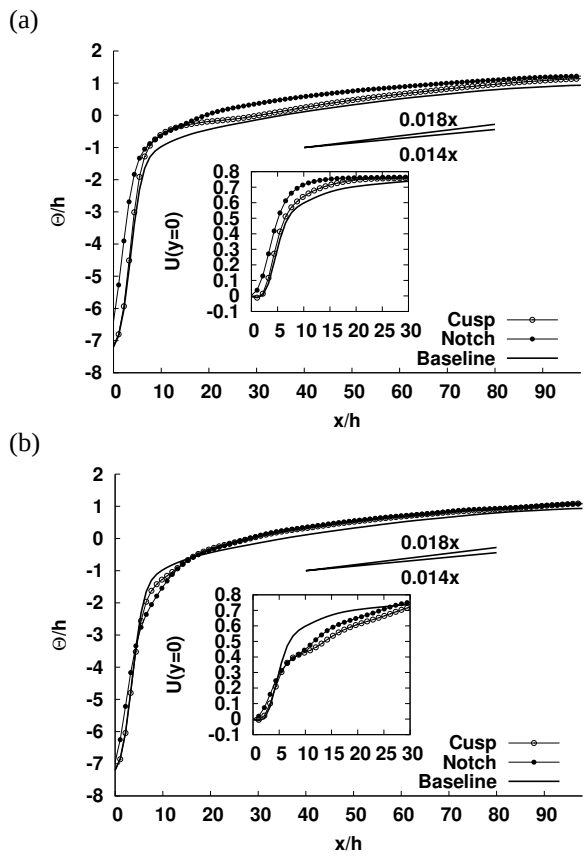

Figure 4: Streamwise evolution of the momentum thickness and (insert) evolution of the mean streamwise velocity downstream of the thick trailing edge, for (a) $\lambda_c = 4.5h$ and (b) $\lambda_c = 3.375h$.

centreline, computed as the minimum of streamwise velocity component at a given vertical plane. Two distinct behaviour are observed: for the largest wavenumber λ_c, the momentum thickness is markedly higher than for the baseline case, with flow downstream of both notch and cusp rising quicker. An interesting behaviour, from $x = 15h$ to $x = 30h$ is observed, where θ, downstream of the chevron's cusp, is actually growing slower than the other two curves. This is attributed, according to Kit et al. (2007) to a region where the flow becomes neutrally stable to the imposed harmonic perturbation. This assertion will be explained later. From $x = 30h$, the "excited" flows follow a quasi-linear evolution. The slope of θ/h is between 0.014 and 0.018, consistent with results found by Kit et al. (2007). The velocity deficit is very different from that of the baseline case (Figure 4, insert), with a much slower recovery for the short wavelength case. This does not translate however, in a different growth rate. Overall, the effect of the chevron is still present up to the end of the computational domain.

The streamwise evolution of both θ and y_{min} for the thin trailing edge (Figure 5) shows that there are very little differences between the baseline, cusp and

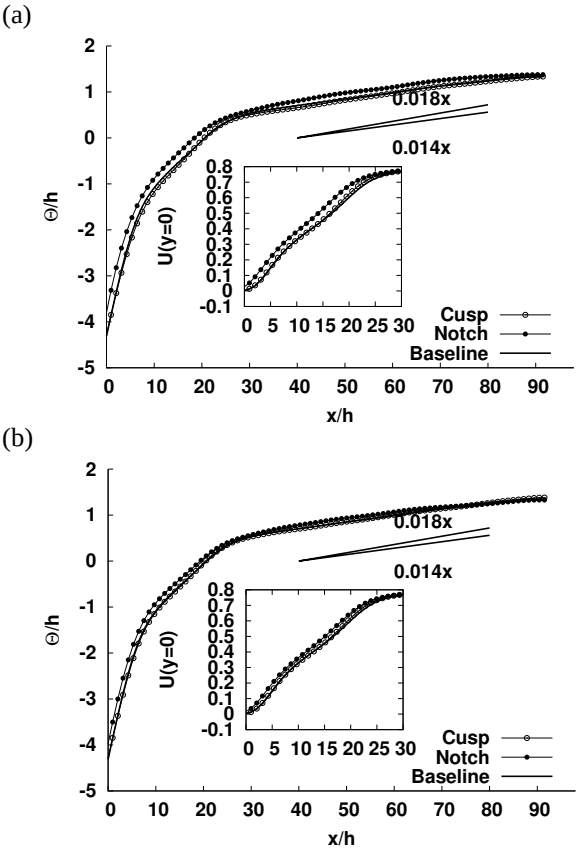

Figure 5: Streamwise evolution of the momentum thickness and (insert) evolution of the mean streamwise velocity downstream of the thin trailing edge, for (a) $\lambda_c = 4.5h$ and (b) $\lambda_c = 3.375h$.

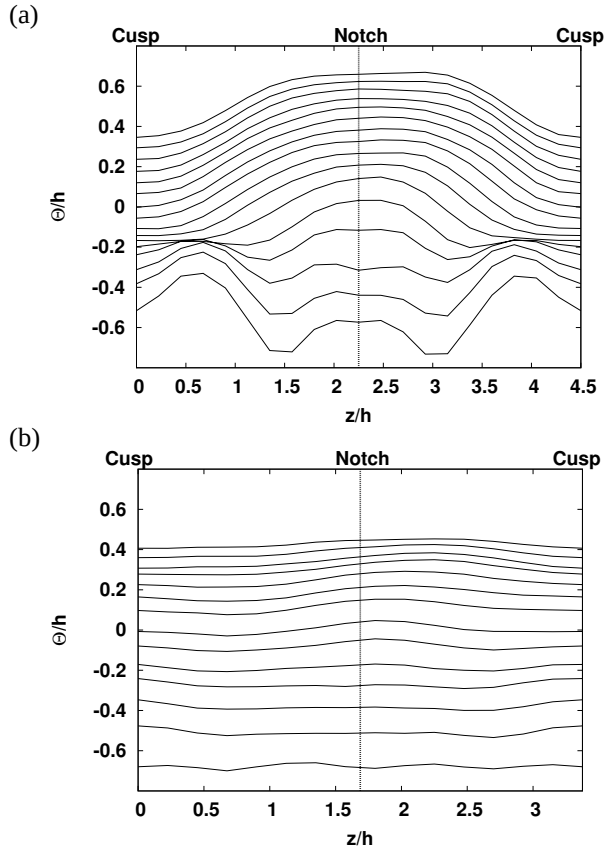

Figure 6: Spanwise profiles of θ/h, for x/h varying from 10 to 40. The lowest curves corresponds to the position closest to the trailing edge (a) $\lambda = 4.5h$ and (b) $\lambda = 3.375h$.

notch planes, with a growth rate similar to the baseline case. The shift observed for the flow in the notch plane can be explained by the difference of origin (the mixing layer is created slightly upstream), however it seems that this difference remains throughout the domain, while the flow becomes very three-dimensional, and seems to be dominated by a translative instability.

Further information, regarding the three-dimensionality of the flow, can be seen in Figure 6, which shows the spanwise profiles of θ/h, for consecutive streamwise positions, and for one chevron only. Near the trailing edge, three peaks are observed, and corresponds to the region of generation of counter-rotating vortices (see below). As the flow evolves, the strong deformation induced by the jagged partition is still present. The smaller thickness is found downstream of the cusp, while the maximum is found at the notch plane. This peculiar behaviour was attributed, by several authors, to an excitation of the instability responsible for the bulging of the Kelvin Helmholtz vortices. This feature is more marked for the larger spanwise spacing, but can still be found for $\lambda = 3.375h$.

Cross-stream velocity and Reynolds-stress profiles, for two different streamwise locations ($x = 10h$ and $x = 40h$) are shown on Figures 7 and 8. The differences observed on θ, which is an integrated value, can be explained clearly. There is a strong asymmetry between the low- and high-speed flow, both at the notch and the cusp. Close to the cusp, the wake-deficit vanishes slowly, while downstream of the notch (not taking into account the shift of origin), the wake deficit has already disappeared, and the profiles is skewed towards the high-speed side. Further downstream, the skewing of the velocity profiles downstream of the notch towards the high-speed side is enhanced, while the opposite effect is found downstream of the cusp: the profiles is skewed on the low-speed side. This can be seen in parallel with the vertical velocity, which can be seen as a characteristic of the flow entrainment. $10h$ downstream of the cusp, the velocity tends to go downwards (Figure 7b), while the flows goes upwards. For both cases, the upward and downward motions are much higher than those found for the baseline case, and explain the strong deformation of the θ-line on Figure 6. Similar observations can be made for $\lambda_c = 3.375h$, but the effect vanishes quickly. For both cases, the Reynolds-stress profiles are skewed, in

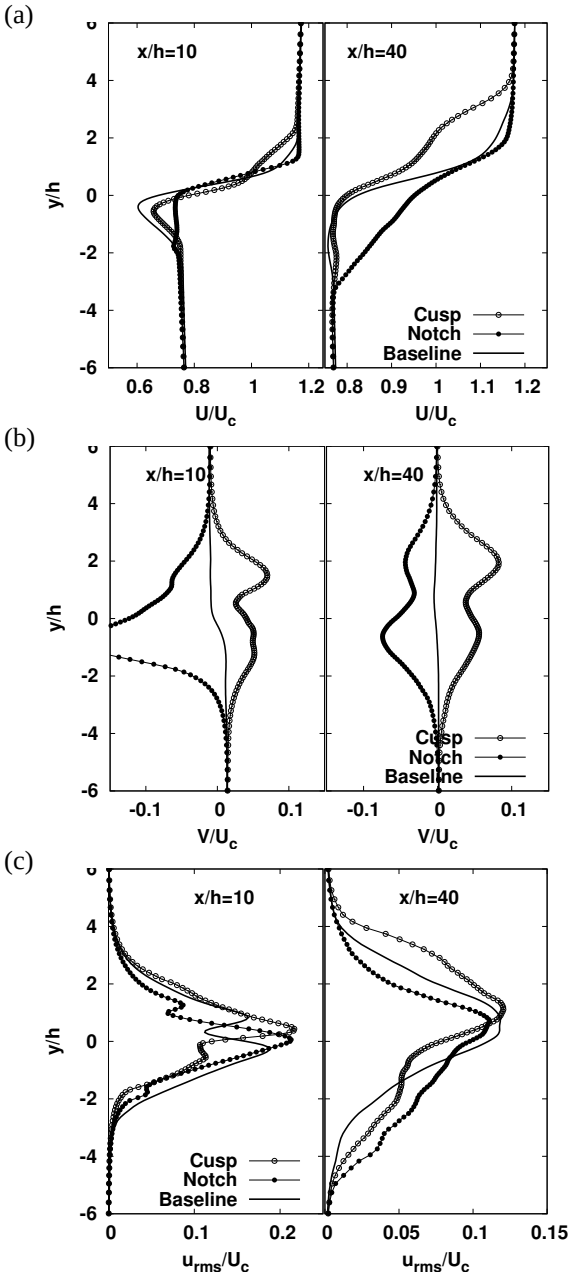

Figure 7: Cross-stream profiles for (a) streamiwse velocity, (b) cross-stream velocity component and (c) streamwise rms-profile, for two different positions, thick trailing-edge, $\lambda_c = 4.5h$.

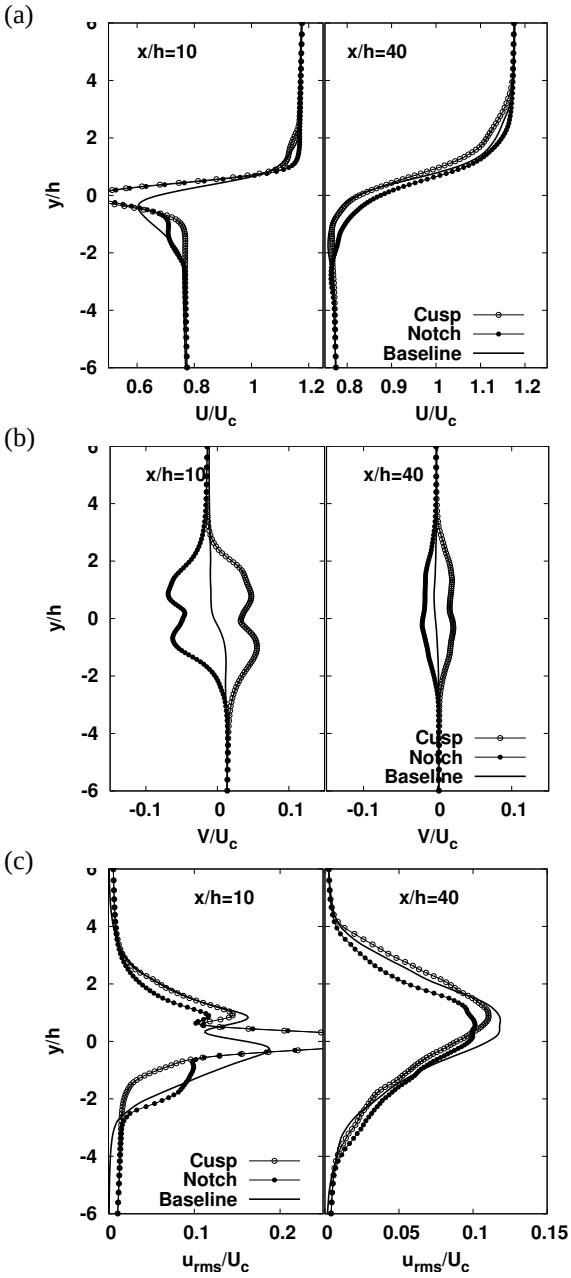

Figure 8: Cross-stream profiles for (a) streamiwse velocity, (b) cross-stream velocity component and (c) streamwise rms-profile, for two different positions, thick, trailing-edge, $\lambda_c = 3.375h$.

the direction of the upward/downward motion.

Plane views of the mean streamwise vorticity ω_x in a plane normal to the flow direction, and for different streamwise positions, are shown on Figures 9 and 10. Streamwise locations for the three planes are shown with white lines on Figure 2. Intense streamwise vortices are created inside the boundary layer on both sides of the flat plate. Then, the counter-rotating vortices increase in strength as the flow evolves downstream, increasing the momentum exchange with the irrotational fluid outside the shear-layer. The streamwise vortices are more intense on the low speed side, and are more intense for the larger chevrons (Figure 9).

5 Conclusion

Direct Numerical Simulations of a spatially developing mixing layers have been conducted. The influence of streamwise vortices in the early stage of the development of the mixing layer is studied by imposing a jagged partition, which is known to enhance mix-

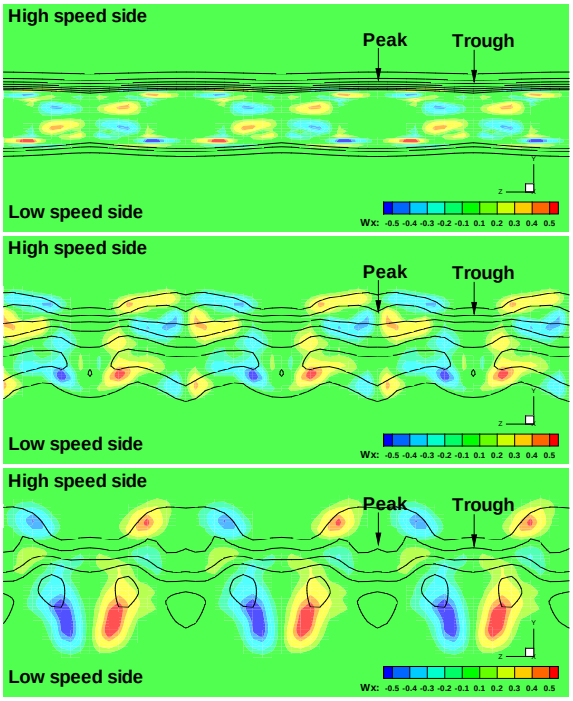

Figure 9: Isocontours of the mean streamwise component of the vorticity on planes normal to the flow direction, for, from top to bottom, $x/h = 0$, 5 and 10, respectively, for the blunt trailing-edge, $\lambda_c = 4.5h$.

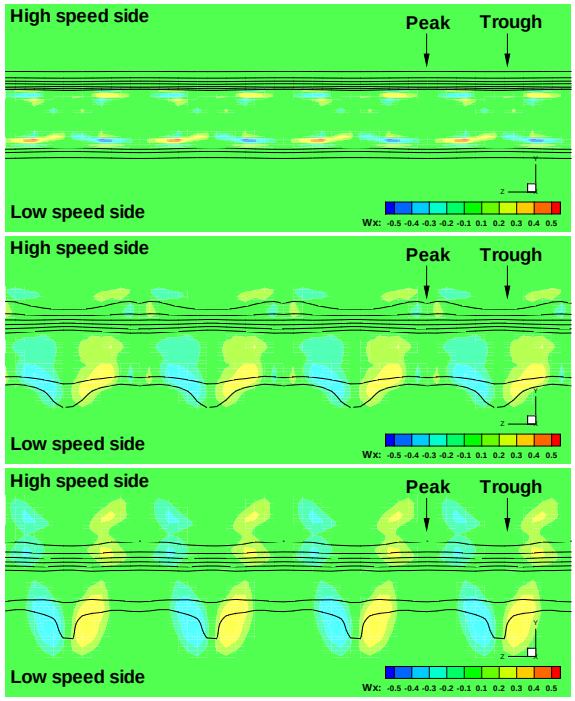

Figure 10: Isocontours of the mean streamwise component of the vorticity on planes normal to the flow direction, for, from top to bottom, $x/h = 0$, 5 and 10, respectively, for the blunt trailing-edge, $\lambda_c = 4.5h$.

ing, and leads to different types of instabilities. The splitter plate is explicitly taken into account by using Immersed Boundary Methods. Four combination of trailing-edge geometries have been studied, using two spanwise spacings for the chevrons, and two trailing edge thicknesses: thin or thick. The effect of a jagged partition is found to be very weak for the thin trailing edge, at least for the wavelength studied. It was however found that the translative instability can be slightly enhanced by using such device (note: the spanwise spacing of the chevrons was of the order of the natural spacing of braids in the non-modified mixing layer). For the thick trailing edge, the strongest effect was found for a rather long wavelength. For this particular trailing-edge geometry, the counter-rotating vortices are found to be very active, on both sides of the splitter plate. Two different evolutions are observed: close to the trailing edge, the counter-rotating vortices bring higher momentum fluid into the region of velocity deficit, explaining the much more rapid thickness growth compared to the baseline case. Further downstream the counter-rotating vortices are still present, but their effect is reversed: they bring high-momentum fluid into the mixing layer from the high-speed side, while extracting momentum on the low-speed side. The work will now focus on the effect of such streamwise vortices on the small-scale mixing.

References

E. Kit, I. Wygnanski, D. Friedman, O. Krivonosova and D. Zhilenko. On the periodically excited plane turbulent mixing layer, emanating from a jagged partition. *J. Fluid Mech.*, **589**, 479–507, 2007.

E. Kit and I. Wygnanski. On periodically excited turbulent mixing layer created downstream of a plane Chevron partition. *Phys. Scripta*, **132** 014008, 2008.

Lasheras, J.C. and Choi, H. Three-dimensional instability of a plane free-shear layer: an experimental study of the formation and evolution of streamwise vortices. *J. Fluid Mech.*, **189**, 54–86, 1988.

S. Laizet, S. Lardeau and E. Lamballais. Direct Numerical Simulation of a mixing-layer downstream a thick splitter plate. *Phys. Fluids*, Vol 22, 015104, 2010.

S. Laizet and E. Lamballais. High-order compact schemes for incompressible flows: A simple and efficient method with quasi-spectral accuracy. *J. Comp. Physics*, **228**(16), pp. 5989-6015, 2009.

P. Parnaudeau, J. Carlier, D. Heitz and E. Lamballais. Experimental and numerical studies of the flow over a circular cylinder at Reynolds number 3 900. *Phys. Fluids*, **20**, 085101.

Schoppa, W., Hussain, F. and Metcalfe, R.W. A new mechanism of small-scale transition in a plane mixing layer: core dynamics of spanwise vortices. *J. Fluid Mech.*, **243**, 183–226, 1995.

Wallace D. and Redekopp L. G. Linear instability characteristics of wake-shear layers, *Phys. Fluids A*, **4**, 189, 1992.

B. Zakharin, E. Kit and I. Wygnanski. On a turbulent mixing layer created downstream of a "Λ" notch simulating one wavelength of a chevron nozzle, *Flow, Turbulence and Combustion*, DOI:10.1007/s10494-009-9217-z, 2009.